

Active Learning of Discrete-Time Dynamics for Uncertainty-Aware Model Predictive Control

Alessandro Saviolo¹, Jonathan Frey², Abhishek Rathod¹, Moritz Diehl², and Giuseppe Loianno¹



Figure 1: By combining online learning with uncertainty-aware model predictive control, the learned dynamics actively adapt to multiple challenging operating conditions, enabling unprecedented flight control.

Abstract—Model-based control requires an accurate model of the system dynamics for precisely and safely controlling the robot in complex and dynamic environments. Moreover, in presence of variations in the operating conditions, the model should be continuously refined to compensate for dynamics changes. In this paper, we propose a self-supervised learning approach to actively model robot discrete-time dynamics. We combine *offline* learning from past experience and *online* learning from present robot interaction with the unknown environment. These two ingredients enable highly sample-efficient and adaptive learning for accurate inference of the model dynamics in real-time even in operating regimes significantly different from the training distribution. Moreover, we design an uncertainty-aware model predictive controller that is conditioned to the aleatoric (data) uncertainty of the learned dynamics. The controller *actively* selects the optimal control actions that (i) optimize the control performance and (ii) boost the online learning sample efficiency. We apply the proposed method to a quadrotor’s system in multiple challenging real-world experiments. Our approach exhibits high flexibility and generalization capabilities by consistently adapting to unseen flight conditions, while it significantly outperforms classical and adaptive control baselines.

Index Terms—Model Learning for Control, Aerial Systems.

SUPPLEMENTARY MATERIAL

Video: <https://youtu.be/QmEhSTcWob4>

I. INTRODUCTION

MODEL-BASED control is an attractive framework for robot control thanks to its adaptivity, scalability, and sample efficiency [1]–[3]. However, it requires access to an accurate model of the system dynamics that is often hard to obtain. For example, an accurate dynamical model for an aerial vehicle requires capturing the highly nonlinear effects generated by aerodynamic forces and torques, propeller interactions, and

vibrations, which cannot be easily modeled [4]. Moreover, in presence of variations in the operating conditions (e.g., the platform may be extended with cable-suspended payloads that would significantly change the dynamics by varying mass and moment of inertia - Figure 1), it is critical to continuously refine the model online. Overall, failing to model such system changes would result in significant degradation of the control performance and may cause catastrophic failures.

Classic modeling of the system dynamics is performed using physics-based principles [5]–[7]. While these approaches can precisely identify rigid-body systems, they fail to represent complex non-linear phenomena, such as friction, deformation, aerodynamic effects, and vibrations, that cannot be directly measured and therefore do not have explicit analytic equations. To circumvent this issue, recent works have investigated data-driven approaches for modeling robot dynamics with different learning paradigms, from offline [8]–[10] to online [11]–[13] and active learning [14]–[16]. Offline learning is the setting where the dynamics model is trained over a set of demonstration data previously collected. Therefore, this learning approach ensures both training over the entire data (i.e., capturing a global dynamical model of the system) and learning without posing any physical risk to the robot. However, offline learning assumes that the global model will remain accurate over time and therefore cannot deal with varying operating conditions that characterize most real-world environments. Online learning extends offline learning by continuously adapting the model during operation with new collected data, thus relaxing the need for a perfect system prior. However, this learning strategy treats the learned model as a passive recipient of data to be processed, hence ignoring the ability of the system to act and influence the operating environment for effective data gathering. Active (online) learning studies the model’s ability to actively select actions to influence what data to learn from [17], [18]. The action selection is performed to maximize a performance gain, such as the maximum entropy [19]. When the actions are selected properly, the model achieves higher sample efficiency.

¹The authors are with Tandon School of Engineering, New York University, New York, USA. e-mail: {as16054, arathod, loiannog}@nyu.edu.

²The authors are with University of Freiburg, Freiburg, Germany. e-mail: {jonathan.frey, moritz.diehl}@imtek.uni-freiburg.de.

In this work, we present a self-supervised learning framework for actively learning discrete-time system dynamics of nonlinear robotic systems. Our approach fully exploits uncertainty-aware Model Predictive Control (MPC) for actively optimizing the control performance and the dynamics learning sample efficiency during operation. The proposed framework is enabled by the following contributions:

- We combine *offline* learning from past experience and *online* learning from present robot interaction with the unknown environment;
- We propose a sample and memory-efficient method inspired by the Unscented Transform (UT) to estimate the aleatoric (data) uncertainty of the learned dynamics;
- We design an uncertainty-aware MPC that leverages the learned dynamics and is conditioned by their corresponding data uncertainty. The controller actively selects the control actions to maximize (i) the control performance and (ii) online learning sample efficiency;
- We experimentally validate the proposed methodology to a quadrotor's system, demonstrating successful adaptation of the learned dynamics in multiple challenging real-world experiments. The dynamical model adapts to substantial system configuration modifications (e.g., cable-suspended payload, propeller mixing) and stochastic external effects (e.g., wind disturbance) unseen during training, enabling unprecedented flight control.

II. RELATED WORKS

The proposed learning approach combines offline and active online learning. In the following, we discuss these techniques to accurately model and adapt robot dynamics.

Offline Learning. Neural Networks (NNs) have been successfully employed for learning robot dynamics due to their favorable expressive power and flexibility [4], [8]–[10] and the simple self-supervised data collection procedure [20], [21]. Similar to previous works, we seek to learn a NN-based model of the system dynamics purely from robot experience. Training the model offline has several advantages compared to pure online learning, such as training without posing any physical risk to the robot and the capability to learn from multiple demonstrations which allows capturing a global model of the system (i.e., the full dynamical evolution of the system). Most of the NN-based approaches, including those related to quadrotor systems, have focused on learning the continuous-time dynamics in a self-supervised manner [4], [8], [10]. However, recovering the ground truth translational and rotational accelerations for training the continuous-time NN-based models is extremely complex due to the highly non-linear sensor noise. Hence, building accurate datasets for training NN-based models for continuous-time dynamics is extremely difficult and error-prone. Conversely, in this work, we propose to directly learn the discrete-time dynamics, bypassing the differentiation step required to recover the unobserved accelerations, similarly to [11]. Consequently, the learned dynamical model is trained over less noisy data and can better generalize to unseen data, as shown in the presented experimental results.

Another popular learning scheme for modeling dynamics offline is meta-learning [22]–[26], which explicitly learns a distribution over different “tasks” (e.g., dynamics associated with different operating regimes). Meta-learning approaches have demonstrated impressive sample efficiency on several tasks, including those considered in this work such as payload transportation [27] and wind disturbance adaptation [13]. However, efficiency is largely obtained by integrating a strong inductive bias over the testing task and often requires huge amounts of data for effective training. Contrarily, the proposed approach is completely task-agnostic, learns offline only a coarse dynamics model from a basic operating regime - alleviating the need for complex hand-designed data sets, and achieves high sample efficiency by actively selecting actions to safely exploit the dynamics model during operation.

Online Learning. In presence of variations in the operating conditions, the dynamics change, and thus the global model learned offline is no longer accurate. Online learning is a promising solution for this issue and consists in continuously updating the model during operation as new data is seen [11]. The optimization can be performed over the whole NN model or only the last layers. Generally, trading-off between these two approaches depends on the similarity of the online and offline training data distributions as well as the available computational budget. When modeling system dynamics, the two distributions are hardly completely dissimilar but share common representations mostly in the deepest dimensions. Moreover, continuously refining the whole model would make it less explainable and thus may yield unexpected predictions. Consequently, in this work, we employ the proposed online learning procedure to only adapt the last layer's weights.

The proposed online optimization procedure is inspired by [28] and [11]. [28] couples model and controller learning by devising a forward loss similar to our formulation. The proposed iterative method allows us to learn an effective control policy on a manipulator and a quadraped in a few iterations. However, the approach is validated using basic system configurations in simulation, hence neglecting all the complex effects that make dynamics modeling a challenging task. Furthermore, such an iterative method would not be feasible in a real-world setting, particularly for an aerial vehicle such as the quadrotor. We solve these two problems by employing an MPC and combining offline and online learning. [11] combines offline and online learning for modeling the dynamics of a manipulator and used MPC for planning under the learned dynamics. The general methodology significantly differs from our approach in terms of optimized objective. Moreover, the authors do not consider the aleatoric uncertainty of the learned dynamics to condition the controller. Hence, the controller may be overconfident during the adaptation and select poor actions.

Gaussian Processes (GPs) are another attractive class of data-driven models for modeling robot dynamics that can be easily adapted online to new data [12], [29]. However, a major drawback of GP regression is computational complexity. Since these models are non-parametric, their complexity increases with the size of the training set. This implies the need to carefully choose a subset of the fitted data that best represents the true dynamics through data reduction techniques [30]–[32].

However, since the dynamics are unknown, selecting these points might be challenging. Moreover, due to their poor scaling properties, GPs need to explicitly model individual dynamical effects (e.g., drag force [33]). Generally, the computational complexity of these non-parametric models can be reduced by learning the dynamics component-wise [34]. However, this results in the failure to capture the hidden dependencies that bound forces and torques.

Online adaptation resembles adaptive control, which seeks to estimate the model errors online and then reactively account for them at the control level [35]–[38]. However, this method trades off robustness with performance, which leads to sub-optimal flight performance [39]. Moreover, in case an MPC is employed as in [40], the optimization problem is solved by respecting defective dynamics constraints and thus potentially degrading the controller’s predictive performance and accuracy as well as erroneously evaluating the feasibility of additional constraints. Conversely, in this work, we introduce an online learning procedure for continuously adapting the learned dynamics used by the MPC. Consequently, the controller fully exploits its predictive power to generate actions, resulting in superior control compared to adaptive control, as shown in the presented experimental results.

Active Learning. Active learning studies the closed-loop phenomenon of a learner selecting actions that influence what data are added to its training set [17]. When selecting the actions, the learner may seek to achieve different goals. Recent works in active learning of robot dynamics have focused on selecting actions that minimize the model (epistemic) uncertainty, hence directing learning gradients toward exploring the entire state-control space. After a globally accurate model of the system dynamics is obtained, the controller fully exploits the learned model to perform the actual task [41]. While this procedure is well-suited for robots that operate in quasi-static operating regimes, it is not practical for systems with highly-nonlinear dynamics and fast varying operating conditions such as aerial vehicles. The continuously changing dynamics would never allow the exploration stage to converge. Moreover, this exploration-exploitation strategy may not reasonably be achievable by parametric models (e.g., NNs, which can potentially require an infinite number of points to model the entire state-control space). In practice, parametric models that are continuously adapted online are not required to fully capture an accurate global model of the system to ensure controllability and stability, but should only be precise locally on a subset of the state-control space. Therefore, we propose to actively select actions that directly maximize the control performance by conditioning the learner (MPC) to the data (aleatoric) uncertainty. The conditioned controller continuously exploits the refined dynamical model and chooses “safe” actions, resulting in faster convergence of the online learning optimization as demonstrated by the proposed results.

III. METHODOLOGY

A. Learning Discrete-Time System Dynamics

Consider a dynamical system with state vector $\mathbf{x} \in \mathbb{R}^n$ and control input $\mathbf{u} \in \mathbb{R}^m$. The discrete-time system identification

task requires finding a function $f : \mathbb{R}^n \times \mathbb{R}^m \rightarrow \mathbb{R}^n$ such that $\mathbf{x}_{t+1} = f(\mathbf{x}_t, \mathbf{u}_t)$ at every time step t . We are interested in solving the system identification problem by approximating f using a feed-forward NN $h(\boldsymbol{\theta})$, where $\boldsymbol{\theta} \in \Theta$ are the NN parameters from the space Θ . The system identification problem then becomes finding $\boldsymbol{\theta}$ that minimizes the prediction error of $h(\boldsymbol{\theta})$ over a set of demonstration data. In this setting, the data consists of state-control trajectories with no additional labels. Hence, finding $\boldsymbol{\theta}$ is a self-supervised learning task because of the absence of an external supervisory signal (i.e., no human labeling of data [21]).

In this work, we provide as input to the NN the translational and rotational velocities, the quaternion representation of the robot orientation, and the control input. We do not provide position information as input since we assume the dynamics are position-independent. We recover the change of position information by using explicit Euler integration [42]. We employ the quaternion representation because it allows a singularity-free mapping from the unit sphere S^3 to the group $SO(3)$. However, when employing NNs to predict the system dynamics, the predicted orientation has no guarantee to respect the quaternion algebraic constraints (quaternion’s norm can become non-unit, and thus may induce non-orthogonal column vectors in the corresponding rotation matrix). This may cause undesired behaviors at run-time and would negatively affect the control performance. Therefore, we treat the predicted orientation $\hat{\mathbf{q}}$ as a non-unit quaternion and map it to a rotation matrix

$$\hat{\mathbf{R}} = \frac{\mathbf{Q}}{\|\hat{\mathbf{q}}\|_2^2},$$

where \mathbf{Q} is defined in [43]. The matrix $\hat{\mathbf{R}}$ can then be converted to any orientation representation, e.g. a unit quaternion.

B. Online Optimization of Learned Dynamics

In presence of variations in the operating conditions, the dynamics change, and the model learned offline is no longer accurate. Therefore, we derive an online optimization strategy that leverages the model learned offline as prior and continuously refines it to the most recent state-control observations.

We control the robot by employing a model-based controller (MPC as detailed in Section III-D) that at each time step calculates the next control action to apply to the system using a dynamics model. If the model is inaccurate, it will lead to inaccurate predictions internally and degrade the control performance. To assess the model quality independently of the employed controller, we define the mismatch between the forward simulation of the dynamics model and the next state as *forward error*. Formally, we define the forward error as

$$\mathcal{L}(\hat{\mathbf{x}}_t, \hat{\mathbf{x}}_{t-1}, \mathbf{u}_{t-1}) = \|\hat{\mathbf{x}}_t - h(\hat{\mathbf{x}}_{t-1}, \mathbf{u}_{t-1}; \boldsymbol{\theta})\|_2^2, \quad (1)$$

where $\hat{\mathbf{x}}_t$ is the state estimate at time t and \mathbf{u}_{t-1} is the action applied at the previous time step. We propose to use the forward error to continuously update the neural dynamics model (Figure 2). The forward error captures all the inaccuracies of the dynamics and is agnostic to the model-based control policy employed. Consequently, optimizing the forward error directly translates into adapting the dynamics to the current operating regime.

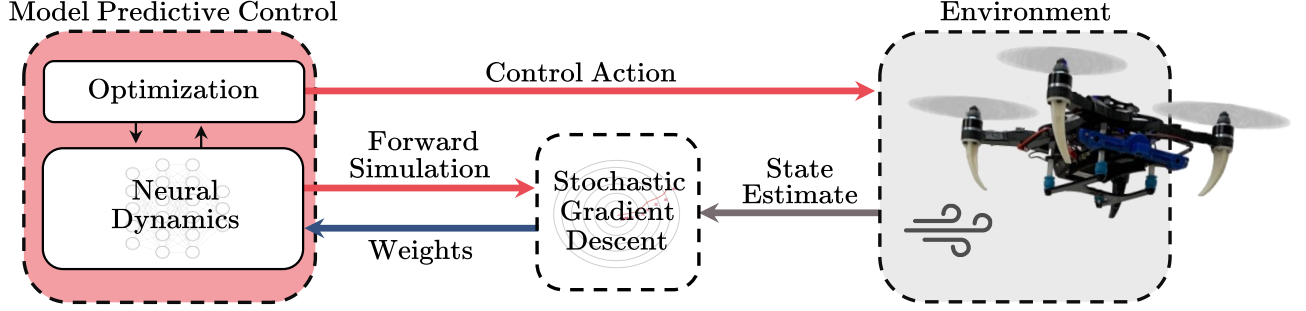


Figure 2: Online learning of the system dynamics. At each control iteration, the neural dynamics are used by the MPC to calculate the next control action to apply to the system and forward simulated to predict the next state. After actuating the predicted action by the controller, the state estimation algorithm provides the actual state reached. Finally, the neural dynamics' weights are updated by using the mismatch between the forward simulated state and the actual state reached by the robot.

We calculate at each control iteration the forward error and use stochastic gradient descent [44] to update the last layer weights of the NN model to minimize it. Formally, let ℓ be the depth of the NN model, then θ can be decomposed into $\theta^1, \dots, \theta^\ell$. Consequently, we can formulate the NN such that

$$h(\mathbf{x}, \mathbf{u}; \theta) = \theta^\ell{}^\top \cdot \phi(\mathbf{x}, \mathbf{u}; \theta^1, \dots, \theta^{\ell-1}), \quad (2)$$

where $\phi(\mathbf{x}, \mathbf{u}; \theta^1, \dots, \theta^{\ell-1})$ represents a feed-forward NN with depth $\ell - 1$ and θ^ℓ is a weight matrix that can be thought of as the last linear layer of $h(\mathbf{x}, \mathbf{u}; \theta)$. The weight update is therefore defined as

$$\theta_t^\ell = \theta_{t-1}^\ell - \eta \frac{1}{B} \sum_{i=t-B}^t \nabla \mathcal{L}(\hat{\mathbf{x}}_i, \hat{\mathbf{x}}_{i-1}, \mathbf{u}_{i-1}), \quad (3)$$

where t is the current control iteration and B defines the batch size. The batch size and learning rate are hyper-parameters that define the NN's ability to adapt and should be carefully chosen. For example, if the environment is significantly affected by external stochastic disturbances or the state estimation is corrupted by noisy spikes, then B should be large to collect more samples while η may be small to take short steps.

Mini-batch optimization offers several key advantages, from alleviating the noisy sensor readings that may lead to uncertain state estimates and thus poor NN updates, to helping stabilize the learning transients that may cause instabilities [45].

C. Uncertainty Estimation of Neural Dynamics

Learning the dynamics purely from data poses the challenge to make the NN and its training process robust to the aleatoric uncertainty caused by noisy sensor measurements. The most important approaches for modeling NNs' uncertainty are Bayesian inference [46], ensemble methods [47], and test time data augmentation [48], [49]. Test time data augmentation methods quantify the predictive uncertainty based on several predictions resulting from different augmentations of the original input sample. In contrast to Bayesian and ensemble methods that rely on ad-hoc architectures or multiple NNs to estimate the uncertainty, test time data augmentation approaches require only one NN for both training and inference, do not need changes on existing NNs, and are not sensitive to the training

process initialization parameters. This motivates us to propose a memory and sample efficient test time data augmentation approach for estimating the dynamics aleatoric uncertainty and condition the MPC optimization formulation to adapt to the model uncertainties.

We employ the UT [50] for calculating the aleatoric uncertainty of the neural dynamics and denote with Σ the corresponding covariance matrix. Given that the previous mean $\bar{\mathbf{x}}_{t-1}$ and covariance Σ_{t-1} matrices are known, the UT is accomplished in three sequential steps: (i) generation of a discrete distribution through sigma points having the same first and second-order moments of the prior data distribution, (ii) propagation of each point in the discrete approximation through the neural dynamics, and (iii) computation of the current mean $\bar{\mathbf{x}}_t$ and covariance Σ_t from the transformed ensemble. Technical details on the uncertainty estimation process and how we address the challenges related to the orientation parameterization that does not belong to the Euclidean space are reported in Appendix -A.

The proposed UT methodology for estimating the dynamics uncertainty is memory and sample efficient since it only stores one model and all the forward evaluations of the sigma points can be efficiently parallelized as in batch training. Moreover, the propagated sigma points capture the posterior mean and covariance accurately up to the 3rd order (Taylor series expansion) for any non-linearity [51].

D. Uncertainty-Aware Model Predictive Control

In the proposed MPC scheme, we formulate the Optimal Control Problem (OCP) with N multiple shooting steps as

$$\begin{aligned} \min_{\substack{\mathbf{x}_0, \dots, \mathbf{x}_N \\ \mathbf{u}_0, \dots, \mathbf{u}_{N-1}}} & \frac{1}{2} \sum_{i=0}^N \tilde{\mathbf{x}}_i^\top \mathbf{Q}_x \tilde{\mathbf{x}}_i + \frac{1}{2} \sum_{i=0}^{N-1} \tilde{\mathbf{u}}_i^\top \mathbf{Q}_u \tilde{\mathbf{u}}_i \\ \text{s.t.} & \quad \mathbf{x}_{i+1} = h(\mathbf{x}_i, \mathbf{u}_i; \theta), \quad \text{for } i = 0, \dots, N-1 \\ & \quad \mathbf{x}_0 = \hat{\mathbf{x}}_0 \\ & \quad g(\mathbf{x}_i, \mathbf{u}_i) \leq 0 \end{aligned} \quad (4)$$

where $\mathbf{Q}_x, \mathbf{Q}_u$ are positive definite diagonal weight matrices, $\tilde{\mathbf{x}}_i = \mathbf{x}_{\text{des},i} - \mathbf{x}_i$ and $\tilde{\mathbf{u}}_i = \mathbf{u}_{\text{des},i} - \mathbf{u}_i$ are the errors between

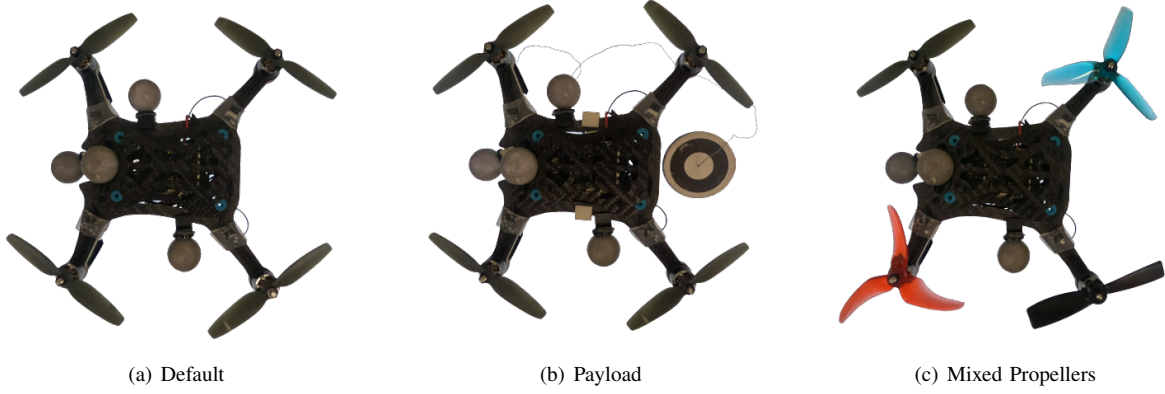


Figure 3: Quadrotor system configurations used in this work. Payload (b) extends Default (a) with a cable-suspended payload that introduces a static model mismatch due to the mass increase and stochastic effects due to the unknown payload swinging motion. Mixed Propellers (c) critically changes Default (a) by using 4 different propellers with various blade compositions.

the desired state and input and the actual state and input. The desired control inputs are obtained from the flat outputs of a differential-flatness planner [52], [53]. The system dynamics are represented by $h(\mathbf{x}_i, \mathbf{u}_i; \boldsymbol{\theta})$ and the initial state is constrained to the current estimate $\hat{\mathbf{x}}_0$. The problem is further constrained by state and input constraints $g(\mathbf{x}_i, \mathbf{u}_i) \leq 0$ which comprise actuator constraints [54].

At each control iteration at time t , the mean $\bar{\mathbf{x}}_{t-1}$ and covariance $\boldsymbol{\Sigma}_{t-1}$ matrices of the state distribution are forward propagated in time as described in Section III-B. Then, the cost matrix \mathbf{Q}_x in (4) is adjusted by the neural dynamics uncertainty and updated as

$$\mathbf{Q}_x \leftarrow \mathbf{Q}_x \text{diag}^{-1}(\boldsymbol{\Sigma}_t), \quad (5)$$

where diag^{-1} is the inverse of the matrix diagonal. The heuristic allows decreasing the penalty of deviations from the desired trajectory for state components for which the NN predictions show high uncertainty and conversely increases the cost of states deviating from their desired values for which the neural model is relatively confident. Moreover, the heuristic boosts the online learning procedure by making the controller choose safer actions and thus resulting in faster convergence and higher sample efficiency of the model training, as shown in the experimental results.

IV. EXPERIMENTAL SETUP

System. We focus on quadrotor systems for conducting experiments. We choose quadrotors because they are under-actuated mechanical systems with highly-nonlinear dynamics and fast varying flight conditions, thus they pose unique challenges for the system identification task. Specifically, we learn the dynamical system of several quadrotor configurations. The default system configuration (Figure 3a) is a 250 g quadrotor equipped with a Qualcomm[®] Snapdragon[™] board and four brushless motors [7]. We extend the default system configuration with a cable-suspended payload that weights 75 g and has cable length 0.8 m (Figure 3b), hence increasing the system mass by 30%. Moreover, we alter the default system configuration by using 4 different propellers with various blade compositions (Figure 3c).

Dynamical Model. Following the notation introduced in Table I, we describe the quadrotor's dynamical system by the state vector $\mathbf{x} = [\mathbf{p}^\top \mathbf{v}^\top \mathbf{q}^\top \boldsymbol{\omega}^\top] \in \mathbb{R}^{13}$ and control input $\mathbf{u} = [\Omega_0 \ \Omega_1 \ \Omega_2 \ \Omega_3] \in \mathbb{R}^4$. Therefore, the system identification task translates into finding a function $f : \mathbb{R}^{13} \times \mathbb{R}^4 \rightarrow \mathbb{R}^{13}$. We approximate f using a feed-forward NN that consists of 3 dense hidden layers of sizes 64, 32, 32. Each hidden layer is stacked with an ELU activation function [55]. We choose ELU over the more commonly used ReLU because it is continuous, differentiable, and slowly becomes smooth. In particular, the two activation functions are defined as follows

$$\begin{aligned} \text{ReLU}(x) &= \max(0, x), \\ \text{ELU}(x) &= \begin{cases} x & \text{if } x > 0 \\ \alpha(\exp(x) - 1) & \text{if } x \leq 0 \end{cases} \end{aligned}$$

where x is the input to the layer, W, b are the weight, bias that define the layer's parameters, and α is a hyper-parameter. ReLU and ELU are very similar except for negative inputs. While ELU becomes smooth slowly, ReLU sharply smooths. Hence, ELU is better suited for MPC optimization and makes the OCP in (4) computationally easier to solve.

The NN input consists of linear velocity \mathbf{v} , angular velocity $\boldsymbol{\omega}$, orientation \mathbf{q} and control input \mathbf{u} , resulting in a 14×1 tensor. The NN output is the discrete-time dynamic state of the quadrotor consisting of velocities and orientation, resulting in a 10×1 tensor.

We train the NN-based dynamics on the real-world data set previously presented and publicly released by [4]. The dataset consists of 68 trajectories with a total of 58' 03" flight time. We select 6 trajectories for testing (Figure 4) and use the remaining for training. Additional details on the employed data set are reported and illustrated in Appendix -B. We run the training process for 20K epochs using Adam optimizer, batch of 1024 samples, and learning rate 0.001. For the online learning phase, we set the learning rate to 0.0002 and the batch size to 20. The training process is performed using PyTorch, while the update of the weights during the online optimization is conducted in a custom implementation of the NN-based dynamics in C++.

Table I
NOTATION

\mathcal{I}, \mathcal{B}	inertial, body frame
$\mathbf{p} \in \mathbb{R}^3$	position in \mathcal{I}
$\mathbf{v} \in \mathbb{R}^3$	linear velocity in \mathcal{I}
$\mathbf{q} \in \mathbb{R}^4$	orientation with respect to \mathcal{I}
$\boldsymbol{\omega} \in \mathbb{R}^3$	angular velocity in \mathcal{B}
$\Omega_i \in \mathbb{R}$	force produced by the i -th propeller

Table II
ABLATION BASELINES

Name	Uncertainty Awareness	Online Learning
Static	✗	✗
Static+UA	✓	✗
Static+OL	✗	✓
Adaptive	✓	✓

Table III
CONTROL BASELINES

Name	Data-Driven Dynamics	Adaptive Control
Nominal	✗	✗
Nominal+L1	✗	✓
Static (Ours)	✓	✗
Adaptive (Ours)	✓	✓

Control. We control the quadrotor by running the MPC formulated in Section III-D on a laptop computer and sending desired body rates and collective thrust via Wi-Fi to a PID controller running onboard the quadrotor. We formulate the MPC OCP in (4) with $N = 20$ shooting steps, covering the evolution of the system over 1 s. The optimization is solved using sequential quadratic programming and a real-time iteration scheme [56] with its implementation in the `acados` package [57]. The Quadratic Programming (QP) subproblems are obtained using the Gauss-Newton Hessian approximation and regularized with a Levenberg-Marquardt regularization term to improve the controller robustness. The QPs are solved using the high-performance interior-point method in `HPIPM` [58] with full condensing and the basic linear algebra library for embedded optimization `BLASFEO` [59]. The OCP solver has been prototyped using the `acados` Python interface and the problem functions are generated using `CasADi` [60]. However, since `CasADi` builds a static computational graph and postpones the processing of the data, it is not compatible with PyTorch which directly performs the computations using the data. Hence, the learned dynamics using PyTorch can not be directly embedded in the formulated MPC. We solve this issue by implementing our customized version of NN-based dynamics directly in `CasADi` symbolics.

Baselines. We validate the proposed approach against multiple baselines in three different sets of experiments. First, we consider the predictive performance of the learned discrete-time dynamics and compare the proposed NN-based model against the continuous-time baseline proposed in [4]. Specifically, we consider the PI-MLP model that was demonstrated to generate more accurate predictions compared to multiple baselines for the quadrotor’s system identification task, from classical approaches to learning-based methods. We feed the continuous-time baseline with the same input information as the proposed discrete-time approach. The continuous-time baseline outputs the continuous-time dynamics of the quadrotor’s system, i.e. linear acceleration $\dot{\mathbf{v}}$ and angular acceleration $\dot{\boldsymbol{\omega}}$. Then, we discretize the continuous-time solutions by employing the Runge-Kutta 4th-order numerical integration.

Second, we validate the tracking performance of the proposed MPC in Section III-D by controlling our quadrotor to continuously track the testing trajectories illustrated in Figure 4. We ablate the proposed Uncertainty-Awareness heuristic (UA) and Online Learning strategy (OL), resulting in four different control methods as summarized in Table II.

Finally, we validate the proposed approach against multiple baselines for quadrotor control. Specifically, we consider an MPC that leverages a nominal model of the quadrotor as

in [7] (*Nominal*) and the nominal MPC augmented by an L1 adaptive controller as in [61] (*Nominal+L1*). Nominal models the quadrotor’s system dynamics by using nonlinear ordinary differential equations and uses the MPC formulated in Section III-D to control the quadrotor. Our implementation uses the same model parameters as in [7]. The nominal MPC represents a non-adaptive baseline that is highly adaptable to the system (requires only changing the model parameters), physically interpretable (based on equations inspired by physics principles), and computationally efficient (compared to an NN-based model). However, while this baseline can precisely identify the quadrotor’s rigid body, it fails to represent complex non-linear phenomena, such as friction, deformation, aerodynamic effects, and vibrations, that cannot be directly measured and thus do not have explicit analytic equations. Adaptive controllers can be employed for augmenting the MPC predictions and modeling these complex non-linear phenomena. Moreover, adaptive controllers can continuously refine the MPC predictions online, hence overcoming the nominal MPC limitation of being static. In this work, we use the L1 adaptive controller proposed in [61] to augment the nominal MPC baseline, hence obtaining another state-of-the-art baseline for quadrotor control. Literature on adaptive control is vast and dates back to the last century. We choose [61] because it is relatively new, it is applied to quadrotor control, and it is open source¹. Our implementation uses the same parameters as in [61]. Additional details on the baselines are available in the corresponding manuscripts, while a summary of the different control baselines used in this work is reported in Table III.

Metrics. We compare our approach against multiple baselines for dynamics learning and quadrotor control based on the Root Mean Squared Error (RMSE) and the Cumulative RMSE (CRMSE). The error metrics between the true state \mathbf{x} and the predicted state $\hat{\mathbf{x}}$ are formulated as

$$\text{RMSE}(\mathbf{x}, \hat{\mathbf{x}}) = \sqrt{\frac{1}{N} \sum_{i=0}^{N-1} (\mathbf{x}_i - \hat{\mathbf{x}}_i)^\top (\mathbf{x}_i - \hat{\mathbf{x}}_i)},$$

$$\text{CRMSE}(\mathbf{x}_t, \hat{\mathbf{x}}_t) = \sum_{i=0}^t \text{RMSE}(\mathbf{x}_i, \hat{\mathbf{x}}_i),$$

where N is the number of components of the state and t is the number of control iterations from the start of the experiment. The CRMSE allows us to easily analyze the trend of the error function over a certain period, hence it is a well-suited metric for understanding the role of methods that make a continuous optimization over time.

¹<https://github.com/HovakimyanResearch/L1-Mambo>

Table IV
PREDICTIVE PERFORMANCE ON UNSEEN TRAJECTORIES BASED ON RMSE

Trajectory	$\dot{\mathbf{v}}_{\max}$ [m s ⁻²]	$\dot{\boldsymbol{\omega}}_{\max}$ [rad s ⁻²]	Continuous-Time [4]	Discrete-Time (Ours)
Ellipse	5.89	7.34	0.36 ± 0.04	0.17 ± 0.04
WarpedEllipse	9.99	12.76	0.41 ± 0.08	0.31 ± 0.09
Lemniscate	13.14	31.98	0.65 ± 0.16	0.51 ± 0.14
ExtendedLemniscate	7.76	27.95	0.32 ± 0.10	0.25 ± 0.11
Parabola	5.91	6.57	0.25 ± 0.05	0.24 ± 0.04
TransposedParabola	17.86	54.90	0.93 ± 0.11	0.49 ± 0.19

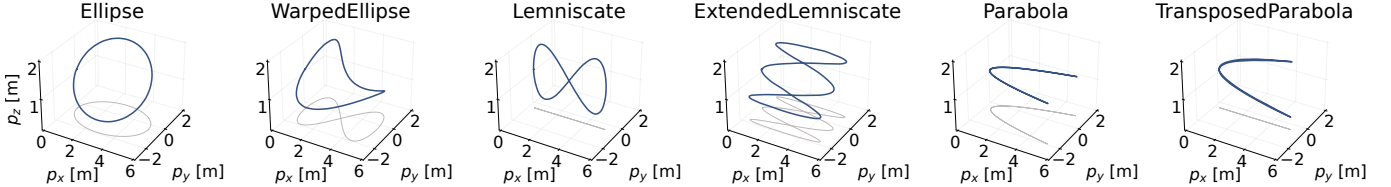


Figure 4: Testing trajectories considered in this work.

V. RESULTS

We design our evaluation procedure to address the following questions. (i) How does the predictive performance of the proposed discrete-time model compare to a continuous-time baseline [4] on real-world data? (ii) What are the benefits of active learning of the dynamics when controlling the quadrotor? (iii) Can the proposed approach adapt to challenging flight regimes and how does it compare against classical [7] and adaptive control baselines [61]? We encourage the reader to consult the video for additional details and results.

A. Discrete vs. Continuous-Time Dynamics

We compare the predictive performance of the proposed dynamics model and a continuous baseline on unseen trajectories collected in the real world (Figure 4). The continuous-time baseline is the model proposed in [4] and was demonstrated to generate more accurate predictions compared to multiple baselines for the quadrotor’s system identification task, from classical approaches to learning-based methods.

Table IV summarizes the results of this experiment. Both models demonstrate excellent performance over all maneuvers, capturing all the complex non-linear effects, and performing accurate predictions. However, despite being trained on the same dataset and sharing a quasi-identical architecture, the proposed model consistently and significantly outperforms the continuous-time baseline, improving the prediction error by up to 50%. The key reason for this dominant performance is the dynamics’ level of abstraction that the model learns. Specifically, learning continuous-time dynamics requires explicitly extracting linear and angular accelerations from flight data. However, this usually simply translates into computing the first-order derivative of velocities that are corrupted by noisy measurements. Hence, the computed accelerations are affected by noisy spikes that limit the learning capabilities of the neural model. Low-pass filters can be applied to minimize the noise in the collected data. However, there is no guarantee that the filters’ outputs are the true dynamics and that the

discarded information is mere noise. Moreover, using filters introduces time delays that may render online learning not effective. Conversely, learning discrete-time dynamics does not require any velocity differentiation and therefore the NN is trained to regress less noisy labels.

B. Leveraging Uncertainty for Control and Dynamics Learning

We demonstrate the role of conditioning the MPC objective function to the aleatoric uncertainty for controlling the quadrotor and boosting the online learning convergence in both simulation and real-world. Table V reports the mean and standard deviation of the positional RMSE when consecutively tracking multiple testing trajectories in simulation. The results show that conditioning the MPC optimization function using the estimated uncertainty infers more stability to the flight controller. Consequently, the uncertainty-aware MPC allows more accurate and precise closed-loop tracking performance compared to the classical MPC, improving the positional RMSE by up to 30%. Moreover, the error plots show that the uncertainty-aware MPC shows better tracking performance over time compared to the classical MPC. Running a fair and accurate comparison between the uncertainty-aware and uncertainty-unaware MPCs requires the use of a simulation environment. However, during simulated flight, the system is not affected by aerodynamic forces and torques, motor dynamics, communication delays, and other non-linear effects that exist in real-world scenarios. Therefore, the aleatoric uncertainty of the dynamical model remains moderate. This results in a similar tracking performance between the uncertainty-aware and uncertainty-unaware MPC during the first seconds of flight. As the flight continues, the tracking error compounds and degrades inevitably the overall performance. This is when the uncertainty-awareness procedure kicks in and improves the overall flight performance.

Figure 5 illustrates the results of this set of experiments when performed in the real world. The results show that the proposed online learning procedure is key for improving the dynamics model continuously over time and enabling

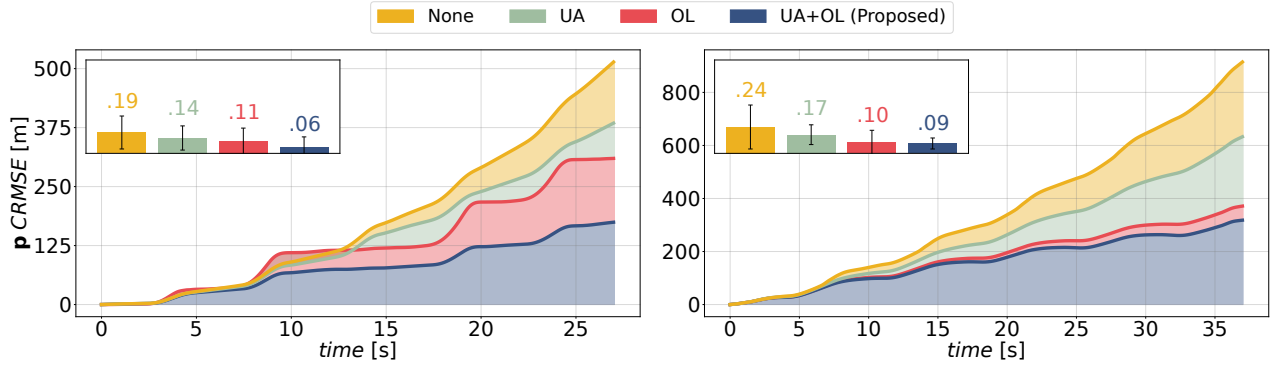


Figure 5: Benefits of combining online learning with uncertainty estimation when continuously tracking WarpedEllipse (left) and Lemniscate (right) trajectories in the real world. The RMSE is accumulated over multiple loops to validate the increased stability introduced by the uncertainty estimation and online optimization. (Inset) Average RMSE over the entire flight performance.

Table V

CLOSED-LOOP TRACKING PERFORMANCE IN SIMULATION

Trajectory	Static	Static+UA
Ellipse	0.29 ± 0.08	0.34 ± 0.10
WarpedEllipse	0.21 ± 0.12	0.23 ± 0.10
Lemniscate	0.12 ± 0.06	0.14 ± 0.09
ExtendedLemniscate	0.09 ± 0.05	0.09 ± 0.06
Parabola	0.20 ± 0.14	0.28 ± 0.12
TransposedParabola	0.14 ± 0.06	0.17 ± 0.06

high-performance control on unseen aggressive trajectories. When the online learning procedure is enabled, the tracking performance of the quadrotor is improved by up to 60%. Moreover, the results demonstrate that conditioning the MPC objective function using the estimated uncertainty enables faster model learning convergence and sample efficiency, hence better-tracking performance over time compared to an uncertainty-unaware controller. When the online learning procedure is enabled and the MPC is conditioned, the tracking performance of the quadrotor is dramatically improved by up to 70%. The key reason for this is that when the MPC is conditioned, it chooses safer actions (i.e., prioritizes tracking certain state components) by favoring exploitation of the dynamics model over exploration and therefore boosts the convergence and sample efficiency of the online model training.

C. Adaptation to Challenging Operating Conditions

We validate the proposed approach in several challenging real-world flight operating conditions, where the quadrotor experiences extensive system configuration modifications or external disturbances. Specifically, we employ the controllers introduced in Section IV and summarized in Table III to control our quadrotor in the following flight operating conditions

- *Payload transportation*: learning the dynamics purely from data poses the challenge to make the NN generalize to domain shifts between training and testing distributions. We study the capability of the proposed approach to adapt to significant changes in the vehicle's mass by attaching to the quadrotor's body a cable-suspended payload with mass 75 g and cable length 0.8 m (Figure 1a). The quadrotor is

required to take off and track a circular trajectory of radius 1 m. Note that the payload not only increases the mass of the quadrotor by 30%, but it also introduces stochastic disturbances due to the payload swing motions;

- *Mixing propellers*: propellers provide lift for the quadrotor by spinning and creating airflow. Mixing different propellers may cause the system to lose stability and fail to track even simple near-hovering trajectories [62]. Therefore, we validate the adaptability of the proposed approach to significant domain shifts by altering the quadrotor's propellers. Specifically, we significantly change the system configuration by using 4 different propellers with various blade compositions (Figure 1b). The quadrotor is required to take off and hover at 0.5 m height;
- *Wind disturbance*: accurate tracking under challenging wind conditions is difficult due to the stochastic nature of wind and the domain shift caused by the new environment dynamics never seen during training. We analyze the adaptability of the proposed approach when an industrial fan blows towards the quadrotor with air speeds up to 3 m s^{-1} (see Figure 1c). The quadrotor is required to take off and hover at 0.5 m height.

Figure 6 illustrates the results of this set of experiments. The results demonstrate that the learned dynamics can be successfully incorporated into an uncertainty-aware MPC framework and combined with an online learning strategy to continuously and actively adapt to multiple challenging flight operating conditions. When extending the system with a cable-suspended payload, non-adaptive controllers (Nominal, Static) struggle to accurately track the desired trajectory, which may lead to fatal navigation failures. Contrarily, augmenting the MPC with an L1 adaptive controller allows to continuously refine the control action to match the unmodelled disturbances and improve the tracking error by 33%. However, this augmentation does not improve the dynamics model leveraged by the MPC, hence the optimization problem is still solved by respecting defective dynamics constraints. Conversely, our approach fully leverages online learning to adapt the NN-based dynamics model to the present flight regime, and thus the MPC predictive power is fully exploited during the controller optimization, resulting in a tracking error reduced by 75% with respect to the Nominal+L1

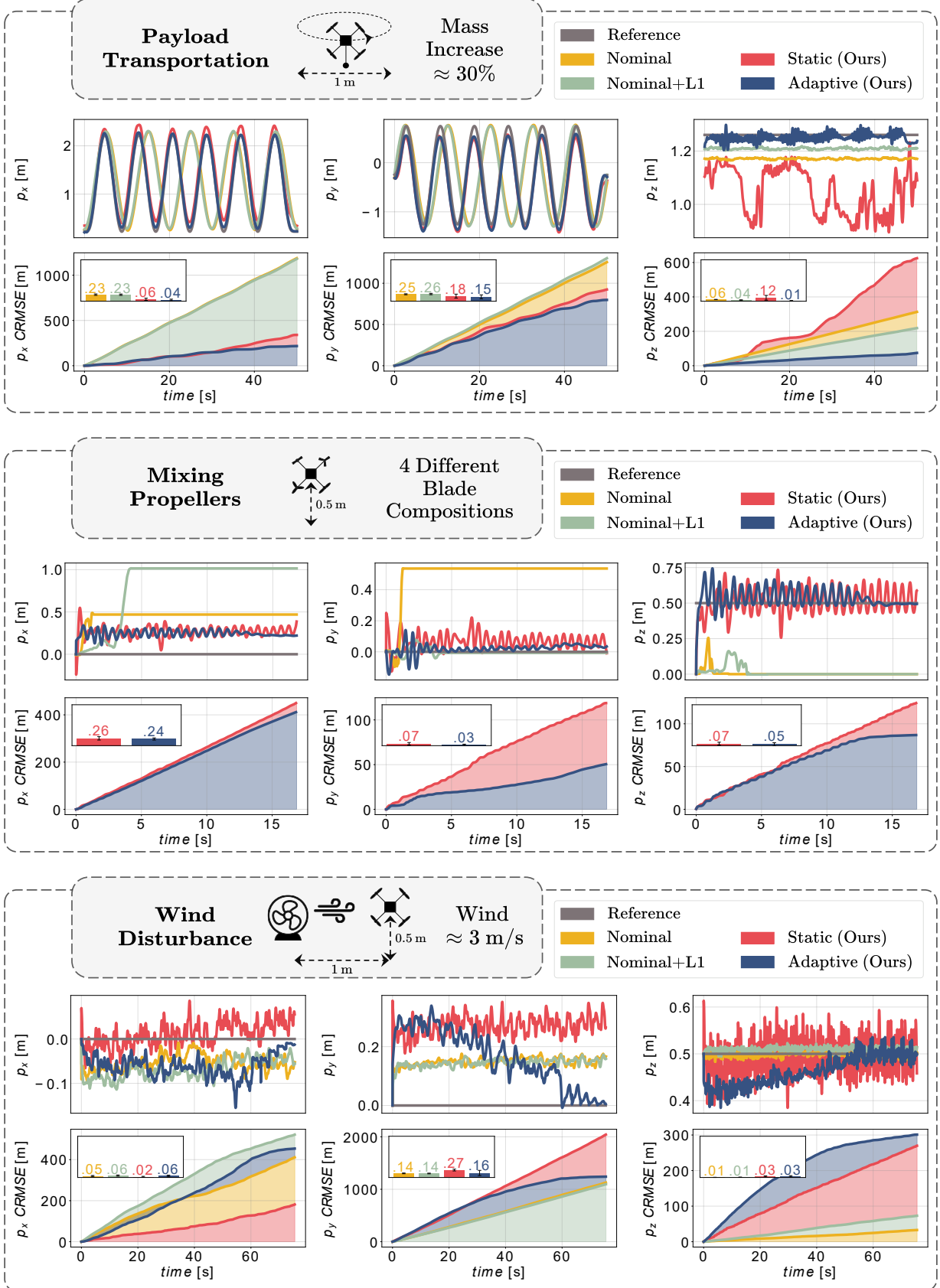


Figure 6: Role of dynamics adaptation in multiple flight operating conditions. (Inset) Average RMSE.

controller and 92% compared to the Static baseline. When mixing different propellers, the quadrotor undergoes severe oscillations and may fail to track even simple near-hovering trajectories, as demonstrated by Nominal and Nominal+L1 flight performance. The Nominal controller heavily relies on an old system model and fails to adapt to the new system dynamics. Consequently, after a few seconds, the quadrotor crashes. L1 adaptive control augments the MPC predicted actions to stabilize the system, however it is still tightly bounded to the old physical dynamics and also leads to a fatal crash. Contrarily, when leveraging NN-based models, the MPC controls the quadrotor to hover close to the desired position. In particular, the Adaptive controller successfully stabilizes the system, hence validating the proposed approach. Interestingly, the learning transient during the adaptation of the NN-based dynamics does not introduce additional oscillations but leads to a stable tracking of the desired position. Accurate tracking under challenging wind conditions is difficult due to the highly stochastic nature of wind that imposes continuous vibrations on the quadrotor, as reflected in the experimental results. When leveraging the physics-based model, the MPC tracks the desired position approximately well. Contrarily, the NN-based dynamics model learned offline struggles to generalize well to the new real-world dynamics and the flight performance of the Static baseline deteriorates compared to the Nominal controller. On the other hand, when employing the proposed Adaptive controller, refining the dynamics model enables the MPC to accurately track the reference state after a minute of online learning, outperforming Nominal even when augmented with an L1 adaptive controller.

VI. DISCUSSION

The experimental results demonstrate that the learned dynamics can be successfully incorporated into an uncertainty-aware MPC framework and combined with an online learning strategy to continuously and actively adapt to static (e.g., changes of mass, mixing of propellers) and stochastic (e.g., payload swings, wind disturbance) model mismatches. At the same time, the results highlight two important aspects of the proposed online optimization strategy.

First, even though the training and testing dynamics distributions are substantially different (Figure 3), the learning transients do not introduce catastrophic oscillations during the online optimization. We consider mini-batch optimization key for this behavior. By leveraging batches of observed state-control pairs, the gradient points in the direction of smooth transitions between different operating regimes. In general, the experimental results show a convergence of the stability of the system (i.e., the controller's initial overshooting is minimized due to a refined dynamics model). This behavior is well illustrated by the mixing propellers experiment and the relative clip in the supplementary video. During the wind disturbance experiments, the stochastic nature of the wind disturbance makes the oscillating behavior difficult to minimize. However, the quadrotor is still able to accurately track the desired trajectory and significantly improve the tracking performance.

Second, during online optimization, the gradient directions strictly depend on the magnitude of the forward error on each

state component. Hence, if the error over a component is much larger than the error over the others, the update of the dynamics model will most likely improve the predictive performance over that component. Sometimes, this may come at the cost of marginally degrading the performance of the other components. However, since this degradation is minimal, this can be considered negligible. For example, during the wind disturbance experiment, the forward error over the y component of the position is much more significant than the error over the other state components. Hence, the online optimization strategy focuses on minimizing the forward error over this component. As a result, despite the stochastic nature of wind that makes the environmental dynamics extremely difficult to model, after about 60 seconds the quadrotor reaches the desired trajectory. Similarly, during the payload transportation experiment, the online optimization successfully minimizes the error over the z component of position due to the mass mismatch. However, in this experiment, the error over the y component of the position is still significantly high. We believe that such an error is related to the stochastic oscillation of the cable-suspended payload. A solution to this problem would be to have extra information in input to the dynamics model about the payload position with respect to the quadrotor [27], hence making the state fully observable [63]. Consequently, the dynamics model would be able to understand if the cable is slack or tilted and find a correlation to its dynamical evolution. However, as we do not provide this information to the dynamics model to maintain a task-agnostic approach, the optimization strategy struggles to optimize the tracking performance over the $x - y$ plane.

VII. CONCLUSION AND FUTURE WORKS

In this work, we presented a novel self-supervised framework for actively modeling quadrotor's discrete-time dynamics. The learned dynamics continuously adapt to multiple challenging flight regimes and operating conditions, enabling unprecedented flight control. Active learning of system dynamics has the potential to terrifically impact the development of multiple robotic systems, enabling fast modeling and high-performance control in multiple operating conditions.

Future Works. The experimental results in Table IV show that the proposed discrete-time dynamics model outperforms a state-of-the-art continuous-time dynamics baseline [4] consistently and significantly in terms of predictive performance. However, the proposed neural dynamics model is currently trained on datasets without taking into account the presence of noisy labels [64]. Future work will focus on investigating novel loss functions for learning with noisy labels and also analyzing the impact of the dataset size on the learned dynamics.

The ablation study illustrated by Figure 5 validates the proposed online learning procedure for enabling high-performance control on unseen aggressive trajectories. Furthermore, the results demonstrate that conditioning the MPC using the estimated uncertainty enables faster model learning convergence and sample efficiency. The proposed uncertainty-awareness heuristic leverages the uncertainty that directly stems from the data. Hence, it does not cover the uncertainty that is caused by shortcomings in the selected dynamics model, namely

the epistemic uncertainty [48]. Future works will extend the proposed heuristic to include epistemic uncertainty, focusing on the errors caused by an insufficient model structure or lack of knowledge due to unknown samples.

The results illustrated in Figure 6 demonstrate that the learned dynamics can be successfully incorporated into an uncertainty-aware MPC framework and combined with an online learning strategy to continuously adapt to challenging operating regimes. While the online learning method showcased impressive performance, it requires a significant amount of time to update the NN weights while concurrently delivering stable control performance. One key reason for this is that the proposed strategy is currently limited by the employed shallow NN's architecture which constraints the method to only update a few weights and biases. Future works will investigate computationally feasible approaches to employ deeper NN architectures that allow both updating a higher number of parameters while still keeping a considerate number of layers frozen. Therefore, the major focus will be put on analyzing the optimal number of layers to update and which sequence of updates to follow.

REFERENCES

- [1] J. Harrison, A. Sharma, R. Calandra, and M. Pavone, "Control adaptation via meta-learning dynamics," in *NeurIPS Workshop on Meta-Learning*, 2018.
- [2] K. Chua, R. Calandra, R. McAllister, and S. Levine, "Deep reinforcement learning in a handful of trials using probabilistic dynamics models," in *Advances in Neural Information Processing Systems*, vol. 31, 2018.
- [3] G. Williams, N. Wagener, B. Goldfain, P. Drews, J. M. Reh, B. Boots, and E. A. Theodorou, "Information theoretic mpc for model-based reinforcement learning," in *IEEE International Conference on Robotics and Automation*, 2017, pp. 1714–1721.
- [4] A. Saviolo, G. Li, and G. Loianno, "Physics-inspired temporal learning of quadrotor dynamics for accurate model predictive trajectory tracking," *IEEE Robotics and Automation Letters*, 2022.
- [5] K. Yoshida and H. Hamano, "Motion dynamics of a rover with slip-based traction model," in *IEEE International Conference on Robotics and Automation*, vol. 3, 2002, pp. 3155–3160.
- [6] P.-B. Wieber, R. Tedrake, and S. Kuindersma, *Modeling and Control of Legged Robots*. Springer International Publishing, 2016, pp. 1203–1234.
- [7] G. Loianno, C. Brunner, G. McGrath, and V. Kumar, "Estimation, control, and planning for aggressive flight with a small quadrotor with a single camera and imu," *IEEE Robotics and Automation Letters*, vol. 2, no. 2, pp. 404–411, 2017.
- [8] L. Bauersfeld, E. Kaufmann, P. Foehn, S. Sun, and D. Scaramuzza, "NeuroBEM: Hybrid Aerodynamic Quadrotor Model," *Robotics: Science and Systems Foundation*, 2021.
- [9] T. Duong and N. Atanasov, "Hamiltonian-based Neural ODE Networks on the SE(3) Manifold For Dynamics Learning and Control," in *Robotics: Science and Systems XVII*, 2021.
- [10] A. Punjani and P. Abbeel, "Deep learning helicopter dynamics models," in *IEEE International Conference on Robotics and Automation*, 2015.
- [11] J. Fu, S. Levine, and P. Abbeel, "One-shot learning of manipulation skills with online dynamics adaptation and neural network priors," *2016 IEEE/RSJ International Conference on Intelligent Robots and Systems (IROS)*, pp. 4019–4026, 2016.
- [12] L. Wang, E. A. Theodorou, and M. Egerstedt, "Safe learning of quadrotor dynamics using barrier certificates," in *IEEE International Conference on Robotics and Automation*, 2018.
- [13] M. O'Connell, G. Shi, X. Shi, K. Azizzadenesheli, A. Anandkumar, Y. Yue, and S.-J. Chung, "Neural-fly enables rapid learning for agile flight in strong winds," *Science Robotics*, vol. 7, no. 66, 2022.
- [14] A. Chakrabarty, C. Danielson, S. D. Cairano, and A. Raghunathan, "Active learning for estimating reachable sets for systems with unknown dynamics," *IEEE Transactions on Cybernetics*, vol. 52, no. 4, pp. 2531–2542, 2022.
- [15] A. Capone, G. Noske, J. Umlauf, T. Beckers, A. Lederer, and S. Hirche, "Localized active learning of gaussian process state space models," in *Proceedings of the 2nd Conference on Learning for Dynamics and Control*, ser. Proceedings of Machine Learning Research, vol. 120. PMLR, 2020, pp. 490–499.
- [16] I. Abraham and T. D. Murphey, "Active learning of dynamics for data-driven control using koopman operators," *IEEE Transactions on Robotics*, vol. 35, no. 5, pp. 1071–1083, 2019.
- [17] D. Cohn, Z. Ghahramani, and M. Jordan, "Active learning with statistical models," *Journal of Artificial Intelligence Research*, vol. 4, pp. 129–145, 1996.
- [18] P. Ren, Y. Xiao, X. Chang, P.-Y. Huang, Z. Li, B. B. Gupta, X. Chen, and X. Wang, "A survey of deep active learning," *ACM Computing Surveys*, vol. 54, no. 9, pp. 1–40, 2021.
- [19] F. Sahli Costabal, Y. Yang, P. Perdikaris, D. E. Hurtado, and E. Kuhl, "Physics-informed neural networks for cardiac activation mapping," *Frontiers in Physics*, vol. 8, 2 2020.
- [20] C. Finn and S. Levine, "Deep visual foresight for planning robot motion," *IEEE International Conference on Robotics and Automation*, pp. 2786–2793, 2017.
- [21] C. Doersch and A. Zisserman, "Multi-task self-supervised visual learning," in *IEEE International Conference on Computer Vision*, 2017, p. 2051–2060.
- [22] C. Finn, P. Abbeel, and S. Levine, "Model-agnostic meta-learning for fast adaptation of deep networks," in *International Conference on Machine Learning*, ser. Proceedings of Machine Learning Research, vol. 70. PMLR, 2017, pp. 1126–1135.
- [23] J. Harrison, A. Sharma, and M. Pavone, "Meta-learning priors for efficient online bayesian regression," in *Algorithmic Foundations of Robotics XIII*. Springer, 2020.
- [24] S. Banerjee, J. Harrison, P. M. Furlong, and M. Pavone, "Adaptive meta-learning for identification of rover-terrain dynamics," *arXiv preprint arXiv:2009.10191*, 2020.
- [25] B. Evans, A. Thankaraj, and L. Pinto, "Context is everything: Implicit identification for dynamics adaptation," in *International Conference on Robotics and Automation*, 2022, pp. 2642–2648.
- [26] A. Nagabandi, I. Clavera, S. Liu, R. S. Fearing, P. Abbeel, S. Levine, and C. Finn, "Learning to adapt in dynamic, real-world environments through meta-reinforcement learning," in *International Conference on Learning Representations*, 2019.
- [27] S. Belkhal, R. Li, G. Kahn, R. McAllister, R. Calandra, and S. Levine, "Model-based meta-reinforcement learning for flight with suspended payloads," *IEEE Robotics and Automation Letters*, vol. 6, no. 2, pp. 1471–1478, 2021.
- [28] S. Bechtel, B. Hammoud, A. Rai, F. Meier, and L. Righetti, "Leveraging forward model prediction error for learning control," in *IEEE International Conference on Robotics and Automation*, 2021.
- [29] L. Hewing, J. Kabzan, and M. N. Zeilinger, "Cautious model predictive control using gaussian process regression," *IEEE Transactions on Control Systems Technology*, vol. 28, no. 6, pp. 2736–2743, 2020.
- [30] S. Ambikasaran, D. Foreman-Mackey, L. Greengard, D. W. Hogg, and M. O'Neil, "Fast direct methods for gaussian processes," *IEEE Transactions on Pattern Analysis and Machine Intelligence*, vol. 38, no. 2, pp. 252–265, 2016.
- [31] J. Quiñero-Candela and C. E. Rasmussen, "A unifying view of sparse approximate gaussian process regression," *Journal of Machine Learning Research*, vol. 6, no. 65, pp. 1939–1959, 2005.
- [32] S. Das, S. Roy, and R. Sambasivan, "Fast gaussian process regression for big data," *Big Data Research*, vol. 14, pp. 12–26, 2018.
- [33] G. Torrente, E. Kaufmann, P. Fohn, and D. Scaramuzza, "Data-Driven MPC for Quadrotors," *IEEE Robotics and Automation Letters*, 2021.
- [34] S. Sarkka, A. Solin, and J. Hartikainen, "Spatiotemporal learning via infinite-dimensional bayesian filtering and smoothing: A look at gaussian process regression through kalman filtering," *IEEE Signal Processing Magazine*, vol. 30, no. 4, pp. 51–61, 2013.
- [35] G. Joshi, J. Virdi, and G. Chowdhary, "Asynchronous deep model reference adaptive control," in *Conference on Robot Learning*, vol. 155, 2021, pp. 984–1000.
- [36] M. Labbadi and M. Cherkaoui, "Robust adaptive nonsingular fast terminal sliding-mode tracking control for an uncertain quadrotor uav subjected to disturbances," *ISA Transactions*, vol. 99, 2019.
- [37] Y. Zou and B. Zhu, "Adaptive trajectory tracking controller for quadrotor systems subject to parametric uncertainties," *Journal of the Franklin Institute*, vol. 354, no. 15, pp. 6724–6746, 2017.
- [38] A. Gahlawat, P. Zhao, A. Patterson, N. Hovakimyan, and E. Theodorou, "L1-gp: L1 adaptive control with bayesian learning," in *Conference on Learning for Dynamics and Control*, vol. 120, 2020, pp. 826–837.

- [39] R. Ortega and E. Panteley, “L1–“adaptive” control always converges to a linear pi control and does not perform better than the pi,” *IFAC Proceedings Volumes*, vol. 47, no. 3, pp. 6926–6928, 2014.
- [40] J. Pravitra, K. A. Ackerman, C. Cao, N. Hovakimyan, and E. A. Theodorou, “L1-adaptive mppi architecture for robust and agile control of multirotors,” *IEEE/RSJ International Conference on Intelligent Robots and Systems*, pp. 7661–7666, 2020.
- [41] T. Lew, A. Sharma, J. Harrison, A. Byland, and M. Pavone, “Safe active dynamics learning and control: A sequential exploration–exploitation framework,” *IEEE Transactions on Robotics*, pp. 1–20, 2022.
- [42] K. E. Atkinson, *An Introduction to Numerical Analysis*, 2nd ed. John Wiley & Sons, 1989.
- [43] C. Rucker, “Integrating rotations using nonunit quaternions,” *IEEE Robotics and Automation Letters*, vol. 3, no. 4, pp. 2979–2986, 2018.
- [44] H. E. Robbins, “A stochastic approximation method,” *Annals of Mathematical Statistics*, vol. 22, pp. 400–407, 2007.
- [45] S. L. Smith, E. Elsen, and S. De, “On the generalization benefit of noise in stochastic gradient descent,” in *International Conference on Machine Learning*, 2020.
- [46] Y. Gal and Z. Ghahramani, “Dropout as a bayesian approximation: Representing model uncertainty in deep learning,” in *International Conference on Machine Learning*, 2016.
- [47] M. Valdenegro-Toro, “Deep sub-ensembles for fast uncertainty estimation in image classification,” *arXiv preprint arXiv:1910.08168*, 2019.
- [48] J. Gawlikowski, C. Tassi, M. Ali, J. Lee, M. Humt, J. Feng, A. Kruspe, R. Triebel, P. Jung, R. Roscher, M. Shahzad, W. Yang, R. Bamler, and X. Zhu, “A survey of uncertainty in deep neural networks,” *arXiv preprint arXiv:2107.03342*, 2021.
- [49] D. Ebeigbe, T. Berry, M. Norton, A. Whalen, D. Simon, T. Sauer, and S. Schiff, “A generalized unscented transformation for probability distributions,” *arXiv preprint arXiv:2104.01958*, 2021.
- [50] E. Goderer, “A quaternion-based unscented kalman filter for orientation tracking,” *International Conference on Information Fusion*, 2003.
- [51] E. Wan and R. Merwe, “The unscented kalman filter for nonlinear estimation,” in *IEEE Adaptive Systems for Signal Processing, Communications, and Control Symposium*, 2000.
- [52] S. Sun, A. Romero, P. Foehn, E. Kaufmann, and D. Scaramuzza, “A comparative study of nonlinear mpc and differential-flatness-based control for quadrotor agile flight,” *IEEE Transactions on Robotics*, pp. 1–17, 2022.
- [53] H. Nguyen, M. Kamel, K. Alexis, and R. Siegwart, “Model predictive control for micro aerial vehicles: A survey,” in *European Control Conference*, 2021, pp. 1556–1563.
- [54] J. Mao, G. Li, S. Nogar, C. Kroninger, and G. Loianno, “Aggressive visual perching with quadrotors on inclined surfaces,” in *IEEE/RSJ International Conference on Intelligent Robots and Systems*, 2021, pp. 5242–5248.
- [55] D. Clevert, T. Unterthiner, and S. Hochreiter, “Fast and accurate deep network learning by exponential linear units (elus),” *arXiv preprint arXiv:1511.07289*, 2016.
- [56] M. Diehl, H. G. Bock, J. P. Schlöder, R. Findeisen, Z. Nagy, and F. Allgöwer, “Real-time optimization and nonlinear model predictive control of processes governed by differential-algebraic equations,” *Journal of Process Control*, vol. 12, no. 4, pp. 577–585, 2002.
- [57] R. Verschuere, G. Frison, D. Kouzoupis, J. Frey, N. van Duijkeren, A. Zanelli, B. Novoselnik, T. Albin, R. Quirynen, and M. Diehl, “acados – a modular open-source framework for fast embedded optimal control,” *Mathematical Programming Computation*, 2021.
- [58] G. Frison and M. Diehl, “HPIPM: a high-performance quadratic programming framework for model predictive control,” *IFAC*, 2020.
- [59] G. Frison, D. Kouzoupis, T. Sartor, A. Zanelli, and M. Diehl, “BLASFEO: Basic linear algebra subroutines for embedded optimization,” *ACM Transactions on Mathematical Software*, 2018.
- [60] J. Andersson, J. Gillis, G. Horn, J. Rawlings, and M. Diehl, “Casadi: a software framework for nonlinear optimization and optimal control,” *Mathematical Programming Computation*, 2018.
- [61] Z. Wu, S. Cheng, K. A. Ackerman, A. Gahlawat, A. Lakshmanan, P. Zhao, and N. Hovakimyan, “L1 adaptive augmentation for geometric tracking control of quadrotors,” *IEEE International Conference on Robotics and Automation*, 2022.
- [62] P.-J. Bristeau, P. Martin, E. Salaün, and N. Petit, “The role of propeller aerodynamics in the model of a quadrotor uav,” in *European Control Conference*, 2009, pp. 683–688.
- [63] A. Markov and N. Nagorny, “Theory of algorithms.” Springer, 1954.
- [64] H. Song, M. Kim, D. Park, Y. Shin, and J.-G. Lee, “Learning from noisy labels with deep neural networks: A survey,” *IEEE Transactions on Neural Networks and Learning Systems*, 2022.
- [65] V. Wüest, V. Kumar, and G. Loianno, “Online estimation of geometric and inertia parameters for multirotor aerial vehicles,” in *IEEE International Conference on Robotics and Automation*, 2019.

APPENDIX

A. Uncertainty Estimation of Neural Dynamics.

Learning the dynamics purely from data poses the challenge to make the NN and its training process robust to the aleatoric uncertainty caused by noisy sensor measurements. Motivated by this observation, we employ the Unscented Transform (UT) [51] for calculating the aleatoric uncertainty of the neural dynamics and denote with Σ the corresponding covariance matrix. Given that the previous mean $\bar{\mathbf{x}}_{t-1}$ and covariance Σ_{t-1} matrices are known, the UT is accomplished in three sequential steps: (i) generation of a discrete distribution through sigma points having the same first and second-order moments of the prior data distribution, (ii) propagation of each point in the discrete approximation through the neural dynamics, and (iii) computation of the current mean $\bar{\mathbf{x}}_t$ and covariance Σ_t from the transformed ensemble.

In this work, we employed the quaternion representation for describing orientations in the group $SO(3)$. Such representation allows a singularity-free mapping from the unit sphere S^3 to $SO(3)$. However, when computing the UT, state vectors need to be summed and subtracted, which is not directly possible when using quaternions because they do not belong to Euclidean space. Therefore, we need to define a procedure for adding and summing quaternions. Following [65], we employ the exponential map (\exp_q) with the quaternion parameterization to commute between a minimal orientation parameterization of rotations, defined as the tangent space at the identity of the Lie group $SO(3)$, and a member of this group

$$\exp_q = e^{q_w} \begin{bmatrix} \cos \|\mathbf{q}_v\| \\ \frac{\mathbf{q}_v}{\|\mathbf{q}_v\|} \sin \|\mathbf{q}_v\| \end{bmatrix}, \quad (6)$$

where $\mathbf{q}_v = [q_x \ q_y \ q_z]$ is the vector part of the quaternion. The logarithm map (\log_q) performs the inverse operation

$$\begin{aligned} \log_q &= \log \left(\|\mathbf{q}\| \frac{\mathbf{q}}{\|\mathbf{q}\|} \right) \\ &= \log \|\mathbf{q}\| + \log \frac{\mathbf{q}}{\|\mathbf{q}\|} \\ &= \log \|\mathbf{q}\| + \mathbf{u}\theta \\ &= \begin{bmatrix} \log \|\mathbf{q}\| \\ \mathbf{u}\theta \end{bmatrix}, \end{aligned} \quad (7)$$

where $\mathbf{v} = \mathbf{u}\theta$, with $\theta = \|\mathbf{v}\| \in \mathbb{R}$ and \mathbf{u} unitary.

To simplify the notation, we introduce the two operators \boxminus, \boxplus to perform the operations $-, +$ between the manifold and the tangent space. We define them as

$$\begin{aligned} \mathbf{q}_1 \boxminus \mathbf{q}_2 &:= 2 \log_q(\mathbf{q}_2^* \otimes \mathbf{q}_1), \\ \mathbf{q} \boxplus \delta &:= \mathbf{q} \otimes \exp_q(\delta/2), \end{aligned} \quad (8)$$

where δ is a vector in the tangent space that represents a rotation around the axis of δ with angle $|\delta|$, $(\cdot)^*$ is the inverse of the quaternion, and \otimes is the quaternion product

$$\mathbf{p} \otimes \mathbf{q} = \begin{bmatrix} p_w q_w - p_x q_x - p_y q_y - p_z q_z \\ p_w q_x + p_x q_w + p_y q_z - p_z q_y \\ p_w q_y - p_x q_z + p_y q_w + p_z q_x \\ p_w q_z + p_x q_y - p_y q_x + p_z q_w \end{bmatrix}. \quad (9)$$

Leveraging the map in (8) and given that the dimensionality of \mathbf{x} is n , we can now detail the UT methodology. We use the covariance matrix $\Sigma_{t-1} \in \mathbb{R}^{n \times n}$ and mean $\bar{\mathbf{x}}_{t-1}$ to get a set $\{\mathcal{X}_{t-1}^{(i)}\}$ of $2n+1$ sigma points,

$$\begin{aligned} \mathcal{X}_{t-1}^{(0)} &= \bar{\mathbf{x}}_{t-1}, \\ \mathcal{X}_{t-1}^{(i)} &= \bar{\mathbf{x}}_{t-1} \boxplus \sqrt{n+\lambda} [\sqrt{\Sigma_{t-1}}]_i, \quad i = 1, \dots, n \\ \mathcal{X}_{t-1}^{(i)} &= \bar{\mathbf{x}}_{t-1} \boxplus \sqrt{n+\lambda} [\sqrt{\Sigma_{t-1}}]_i, \quad i = n+1, \dots, 2n \end{aligned} \quad (10)$$

where $\lambda = \alpha^2(n + \kappa) - n$ depends on hyper-parameters α, κ and determines the sigma points spread, and the square root of the covariance is obtained via Cholesky decomposition.

The state distribution is now represented by a minimal set of carefully chosen sigma points. These points well capture the mean and covariance of the original distribution and can be forward propagated through the neural dynamics to project them ahead of time

$$\mathcal{X}_t^{(i)} = h(\mathcal{X}_{t-1}^{(i)}, \mathbf{u}_{t-1}; \boldsymbol{\theta}), \quad i = 0, \dots, 2n \quad (11)$$

Finally, the posterior mean and covariance can be accurately calculated by using a weighted sample mean and covariance of the posterior sigma points

$$\hat{\boldsymbol{\mu}}_t = \mathcal{X}_t^{(0)} \boxplus \sum_{i=0}^{2n} W_i^{(m)} \left(\mathcal{X}_t^{(i)} \boxminus \mathcal{X}_t^{(0)} \right) \quad (12)$$

$$\hat{\Sigma}_t = \sum_{i=0}^{2n} W_i^{(c)} \left(\mathcal{X}_t^{(i)} \boxminus \hat{\boldsymbol{\mu}}_t \right) \left(\mathcal{X}_t^{(i)} \boxminus \hat{\boldsymbol{\mu}}_t \right)^\top, \quad (13)$$

where W_i is the weight associated with the i -th sigma point defined as

$$\begin{aligned} W_0^{(m)} &= \frac{\lambda}{n + \lambda}, & W_i^{(m)} &= \frac{1}{2(n + \lambda)}, \\ W_0^{(c)} &= \frac{\lambda}{n + \lambda} + (1 - \alpha^2 + \beta), & W_i^{(c)} &= \frac{1}{2(n + \lambda)}, \end{aligned} \quad (14)$$

where β is a hyper-parameter that increases the weight of the mean of the posterior sigma points.

The proposed UT methodology for estimating the dynamics uncertainty is memory and sample efficient since it only stores one model and computes $2n+1$ forward evaluations which can be parallelized as in batch training. Moreover, the propagated sigma points capture the posterior mean and covariance accurately up to the 3rd order (Taylor series expansion) for any non-linearity [51]. The methodology depends on the hyper-parameters α, κ, β . In this work, we set $\alpha = 0.001, \kappa = 1, \beta = 2$ assuming a Gaussian prior distribution.

B. Discrete vs. Continuous-Time Dynamics.

We extend the analysis of discrete and continuous-time dynamics introduced in Section V-A. Specifically, we illustrate the different ground truth data that the NN models are trained on in the two different tasks. Figure 7 and Figure 8 illustrate samples of rotational velocities and accelerations that constitute our and [8] data sets. The rotational velocities are extracted from the IMU sensor and are thus affected by very little noise. Therefore, learning discrete-time dynamics is better suited for the model learning process. In the continuous-time case, the unobserved rotational accelerations are calculated as the first-order derivative of the rotational velocities. Hence, the mild noise affecting the velocities is strongly inflated by the differentiation operation. Despite the low-pass filters that can be employed to reduce the noise, directly training on such noisy labels significantly deteriorates the learning process, leading to a less stable training convergence. This is also demonstrated by the experimental results reported in Section V-A.

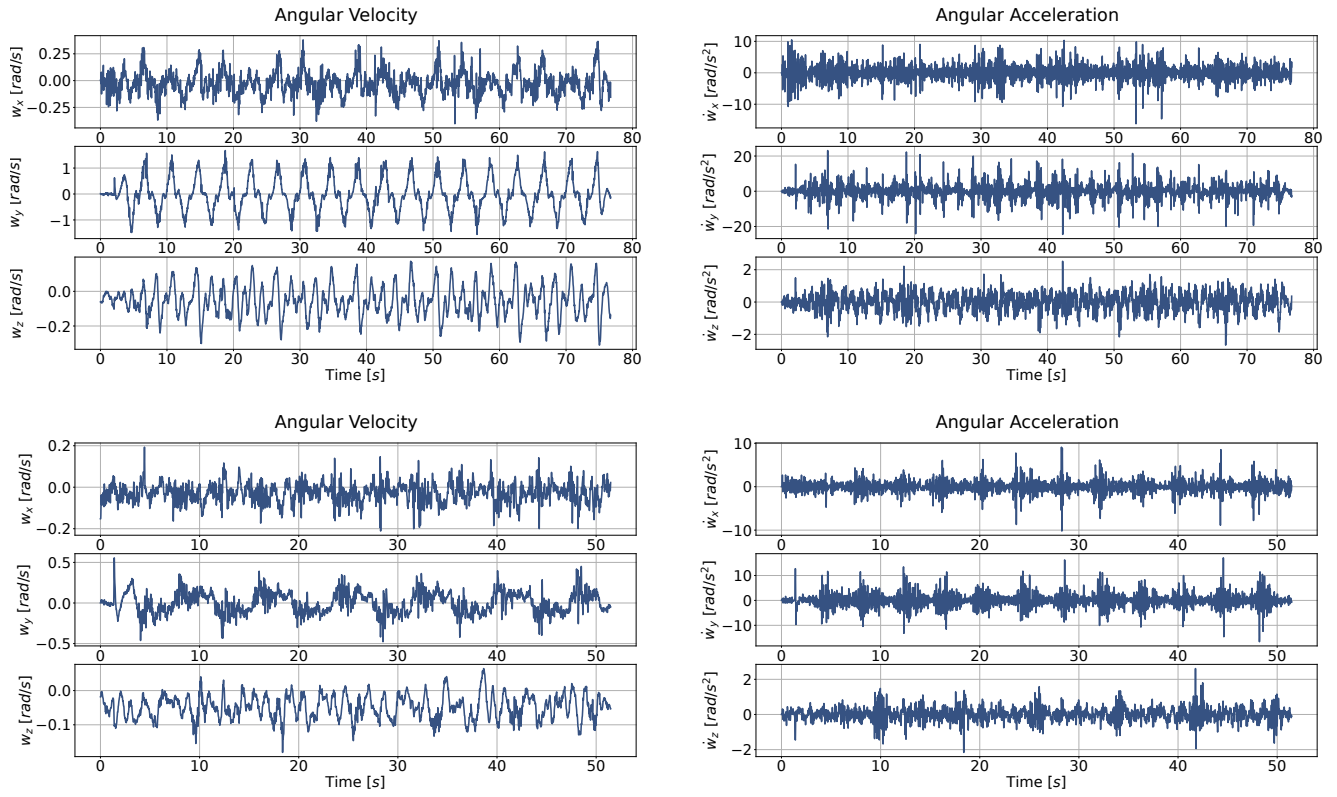


Figure 7: Samples of collected rotational velocities and accelerations from [4] data set.

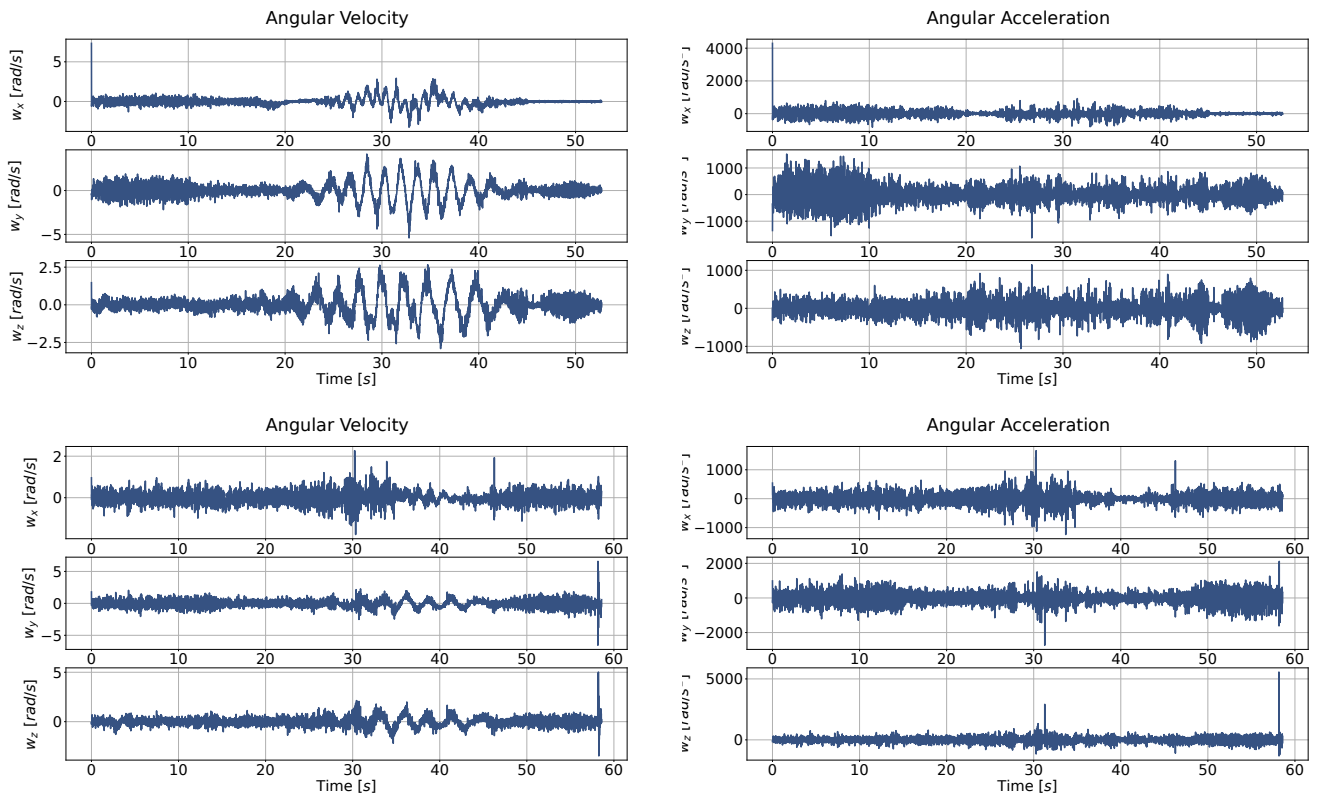


Figure 8: Samples of collected rotational velocities and accelerations from [8] data set.